



Very Slow Rotators from Tidally Synchronized Binaries

David Nesvorný¹ , David Vokrouhlický², William F. Bottke¹, Harold F. Levison¹, and William M. Grundy³

¹Department of Space Studies, Southwest Research Institute, 1050 Walnut Street, Suite 300, Boulder, CO 80302, USA

²Institute of Astronomy, Charles University, V Holešovičkách 2, CZ-18000 Prague 8, Czech Republic

³Lowell Observatory, 1400 West Mars Hill Road, Flagstaff, AZ 86001, USA

Received 2020 February 25; revised 2020 March 21; accepted 2020 March 24; published 2020 April 10

Abstract

A recent examination of K2 lightcurves indicates that $\sim 15\%$ of Jupiter Trojans have very slow rotation (spin periods $P_s > 100$ hr). Here we consider the possibility that these bodies formed as equal-size binaries in the massive outer disk at $\sim 20\text{--}30$ au. Prior to their implantation as Jupiter Trojans, tight binaries tidally evolved toward a synchronous state with $P_s \sim P_b$, where P_b is the binary orbit period. They may have been subsequently dissociated by impacts and planetary encounters with at least one binary component retaining its slow rotation. Surviving binaries on Trojan orbits would continue to evolve by tides and spin-changing impacts over 4.5 Gyr. To explain the observed fraction of slow rotators, we find that at least $\sim 15\%\text{--}20\%$ of outer disk bodies with diameters $15 < D < 50$ km would have to form as equal-size binaries with $12 \lesssim a_b/R \lesssim 30$, where a_b is the binary semimajor axis and $R = D/2$. The mechanism proposed here could also explain very slow rotators found in other small-body populations.

Unified Astronomy Thesaurus concepts: [Kuiper belt \(893\)](#); [Jupiter trojans \(874\)](#); [Tidal interaction \(1699\)](#)

1. Slow Rotators among Jupiter Trojans

Szabó et al. (2017) and Ryan et al. (2017) analyzed the Kepler telescope photometry during K2 Campaign 6 from 2015 July 14 to September 30, and determined spin periods for 56 Jupiter Trojans. Thanks to a nearly continuous photometric coverage of all targets over a 78 day campaign, this data set is not biased against slow rotators. We cross-linked the two data sets to find that the results are generally consistent (Figure 1). In two cases, (13185) Agasthenes and (65240) 2002 EU106, the estimated periods are significantly different (e.g., Ryan et al. finds $P_s = 113$ hr for Agasthenes, whereas Szabó et al. finds $P_s = 11.6$ hr, probably because this object has a very small lightcurve amplitude). We also discarded (39270) 2001 AH11, for which Szabó et al. gives a three times longer period than Ryan et al. In some cases, the periods differ by a factor of two due to ambiguity in the lightcurve phase folding. We include these cases in Figure 1 because they do not affect the classification of Trojans into fast and slow rotators. In total, eight out of 53 Trojans ($\sim 15\%$) have very long spin periods ($P_s > 100$ hr).

Rotation of a small body is set by planetesimal formation processes (Johansen & Lacerda 2010; Visser et al. 2020), and evolves by impacts (Farinella et al. 1992) and radiation effects such as Yarkovsky–O’Keefe–Radzievskii–Paddack (YORP; Vokrouhlický et al. 2003). Formation processes and impacts are expected to yield the Maxwellian distribution (e.g., Medeiros et al. 2018) with predominantly fast spins. The YORP effect was previously suggested to explain the excess of slow rotators among small asteroids (Pravec et al. 2008). We find it unlikely that the YORP effect can explain the very slow rotators in Figure 1. Scaling from the detected YORP acceleration of asteroid Bennu ($d\omega/dt = 2.6 \times 10^{-6}$ rad d $^{-2}$; Nolan et al. 2019) to semimajor axis $a = 5.2$ au and diameter $D = 30$ km, we estimate that it would take ~ 40 Gyr for YORP to change the rotational period from 15 to 500 hr (the YORP timescale scales with $a^2 D^2$; Vokrouhlický et al. 2015). In addition, the two slowest rotators with $P_s > 500$ hr are also the largest ((23958) 1998 VD30 with $D \simeq 46$ km and (13366) 1998 US24 with $D \simeq 33$ km), whereas YORP is the most effective for small

bodies. Adding to that, (11351) Leucus, a $D \simeq 35$ km target of the Lucy mission (Levison & Lucy Science Team 2016), has $P_s = 513.7$ hr (French et al. 2015).

2. Implantation of Jupiter Trojans and Binaries

Current dynamical models suggest that Jupiter Trojans formed in the outer planetesimal disk at $\sim 20\text{--}30$ au and were implanted onto their present orbits after having a series of scattering encounters with the outer planets (Morbidelli et al. 2005; Nesvorný et al. 2013, also see Pirani et al. 2019). The orbital excitation during encounters can explain the high orbital inclinations of Trojans. The formation of Jupiter Trojans at $\sim 20\text{--}30$ au is reinforced by their similarities (e.g., colors, size distribution) to the trans-Neptunian objects (TNOs; e.g., Fraser et al. 2014; Emery et al. 2015; Wong & Brown 2016).

TNOs can be classified into two dynamical categories: cold and hot. The cold population (also called the “cold classical” population), with semimajor axes $a = 42\text{--}47$ au and $i < 5^\circ$, is thought to have formed in situ at >40 au (e.g., Parker & Kavelaars 2010; Batygin et al. 2011). At least 30% (Noll et al. 2008), and perhaps as much as 100% (Fraser et al. 2017), of cold classicals formed as equal-size binaries (e.g., Goldreich et al. 2002; Nesvorný et al. 2010). The equal-size binaries are relatively rare in the hot population (hot classicals, resonant, and scattered; see Gladman et al. 2008 for definitions), probably because wide and thus observable binaries starting at $\sim 20\text{--}30$ au were dissociated by impacts and planetary encounters prior to their implantation into the Kuiper Belt (Petit & Mousis 2004; Parker & Kavelaars 2010).

Some wide equal-size binaries survived in the hot population, suggesting that the initial binary fraction at $\sim 20\text{--}30$ au was high (Nesvorný & Vokrouhlický 2019). The chances of survival are better for tight binaries that are more strongly bound together. These binaries are difficult to observationally detect in the Kuiper Belt (Noll et al. 2008), but can be resolved closer in. For example, (617) Patroclus and Menoetius, a pair of 100 km class Jupiter Trojans, is a binary with $a_b \simeq 670$ km (Marchis et al. 2006). The Patroclus-Menoetius binary evolved by tides into a

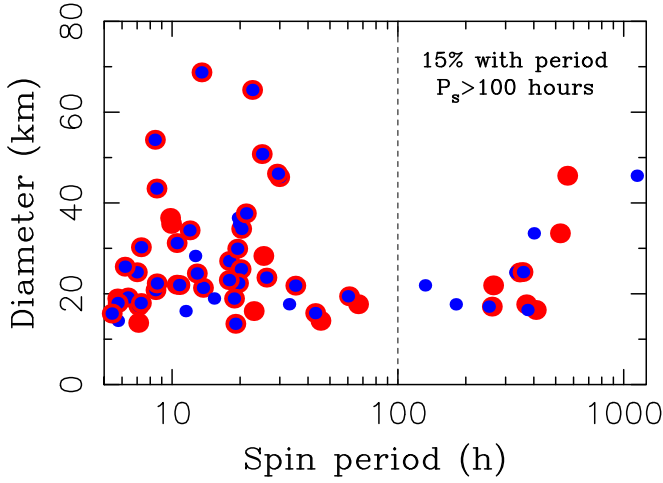


Figure 1. Spin periods of Jupiter Trojans from Ryan et al. (2017; bigger red dots) and Szabó et al. (2017; smaller blue dots). We excluded three cases with inconsistent period determinations (see the main text), leaving 53 objects. We included all cases where the period determination in one work was double the one found in the other work. The period determinations in Ryan et al. and Szabó et al. precisely agree with each other in 40 cases (blue and red dots overlap in the plot).

synchronous state, where the orbital period matches spin periods of both components, $P_s = P_b = 103.5$ hr (Mueller et al. 2010). It is not plotted in Figure 1, but if it were to be, it would contribute to the group of very slow rotators with $P_s > 100$ hr. We are therefore compelled to consider the possibility that the slow rotators among Jupiter Trojans are tidally synchronized binaries (surviving or dissociated).

3. Tidal Synchronization Timescale

For a binary with primary and secondary radii R_1 and R_2 , densities $\rho_1 = \rho_2 (= \rho)$ and masses m_1 and m_2 , the tidal evolution of secondary’s spin is given by

$$\frac{1}{\omega^*} \frac{d\omega}{dt} = -\tau_\omega^{-1}, \quad (1)$$

where

$$\tau_\omega^{-1} = \frac{15}{4} \frac{k}{Q} \left(\frac{R_1}{a} \right)^{9/2} n \quad (2)$$

is the synchronization timescale (Goldreich & Sari 2009). Here, $\omega^* = (Gm_2/R_2^3)^{1/2}$ is the break-up spin rate, G is the gravitational constant, k is the tidal Love number, Q is the tidal quality factor, and n is the orbital frequency. We assume that the spin is prograde and initially fast ($\omega = \omega^* \gg n$). A similar equation holds for the evolution of primary’s spin. The basic problem with using Equation (2) for TNOs or Jupiter Trojans is that the Q/k factor is unknown.

We use observations of TNO binaries to infer this factor. The equal size, 100 km class TNO binaries show a clear trend of binary eccentricity e_b with separation (Figure 2). The binaries with $a_b/R < 55$ have nearly circular orbits with $e_b < 0.03$, whereas the more separated binaries have a wide range of eccentricities. We interpret this trend to be a consequence of tidal circularization. The binary eccentricity evolution due to

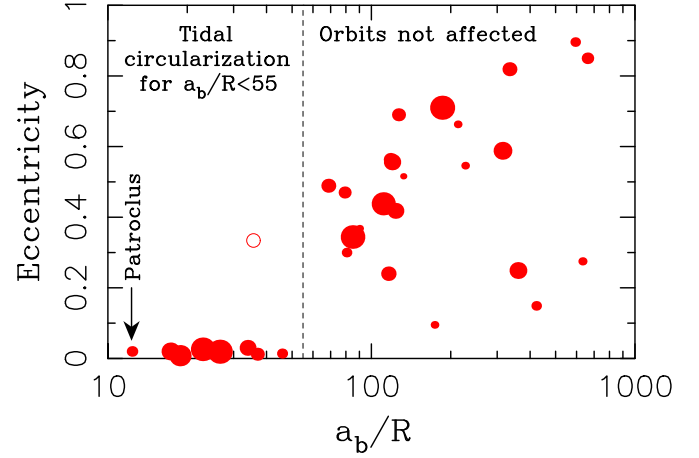


Figure 2. Orbits of Kuiper Belt binaries. We selected 36 binaries from Noll et al. (2020) with $R_1 < 150$ km (to remove dwarf planets) and $R_2/R_1 > 0.5$ (approximately equal size). The binary semimajor axis was normalized by the mean physical radius $R = (R_1 + R_2)/2$, where the primary and secondary radii, R_1 and R_2 , were taken from the Johnston’s archive (Johnston 2018; <https://sbn.psi.edu/pds/resource/binmp.html>), Vilenius et al. (2014), and Stansberry et al. (2012). A similar plot can be obtained if the radii are computed from absolute magnitudes (Grundy et al. 2019; Noll et al. 2020) and albedo $p_V \simeq 0.1$. The size of a symbol is proportional to R_1 (the smallest symbol corresponds to $R_1 = 32$ km of 2000 CF105; the largest to $R_1 = 149$ km of 2002 XH91). The great majority of binaries shown here are cold classicals (30 in total). We do not show Centaur binary (42355) Typhon whose binary eccentricity $e_b = 0.51$ was likely excited by planetary encounters (Nesvorný & Vokrouhlický, 2019). The circle symbol is a hot classical binary 2001 QC298 with a very low albedo $p_V = 0.034$ from Vilenius et al. (2014). It would shift to the right if the actual albedo is higher. The Patroclus-Menoetius binary with a circularized and double synchronous binary orbit is indicated by the arrow.

tides (Goldreich & Sari 2009) is given by

$$\frac{1}{e_b} \frac{de_b}{dt} = -\tau_e^{-1} \quad (3)$$

with the eccentricity damping timescale

$$\tau_e^{-1} = \frac{k}{Q} n \left[\frac{21}{2} \frac{m_1}{m_2} \left(\frac{R_2}{a} \right)^5 - \frac{57}{8} \frac{m_2}{m_1} \left(\frac{R_1}{a} \right)^5 \right], \quad (4)$$

where we assume that the k/Q factor is the same for primary and secondary. Equation (4) strictly applies only for $e \ll 1$. Here we use it as a guide for the timescale on which a binary orbit is circularized.⁴

Figure 3 shows the circularization timescale for known TNO binaries. We find $Q/k \simeq 2500$ such that $\tau_e \simeq 4.5$ Gyr for binaries with $a_b/R = 55$. Using $Q/k \simeq 2500$ in Equation (2) we can estimate how long it takes to reach a synchronous state starting from the critical rotation (Figure 4). As we will see below, the binary lifetime (i.e., the time interval before a binary becomes dissociated by collisions or encounters) depends on the outer disk mass m_{disk} and lifetime t_{disk} . Adopting $m_{\text{disk}} = 20$ Earth masses and $t_{\text{disk}} = 10\text{--}100$ Myr from Nesvorný et al. (2018), we find that binaries with $a_b/R < 30\text{--}45$ should become synchronous. This corresponds to the rotation periods up to 400–750 hr. We thus see that tides are capable of producing very long rotational periods. The surviving binaries on Trojan orbits would evolve by tides over 4.5 Gyr and can become

⁴ We ignore the effect of tides on binary semimajor axis. This effect is small because there is not enough angular momentum contained, relative to the orbital momentum, in the initial spin (even if it is critical).

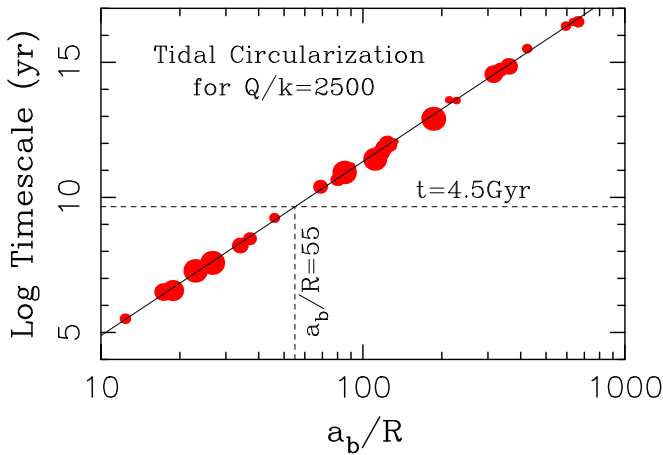


Figure 3. Tidal circularization timescale τ_c of TNO binaries. We compute τ_c from Equation (4) for TNO binaries shown in Figure 2, find the best fit in the log–log space (solid line), and adjust Q/k such that $\tau_c = 4.5$ Gyr for $a_b/R = 55$ (dashed lines). This gives $Q/k = 2500$. To get some sense of the uncertainty of this estimate, we repeat the same calculation for $a_b/R = 50$ and $a_b/R = 60$ obtaining $Q/k = 4000$ and $Q/k = 1500$, respectively. The density $\rho = 1 \text{ g cm}^{-3}$ was adopted here.

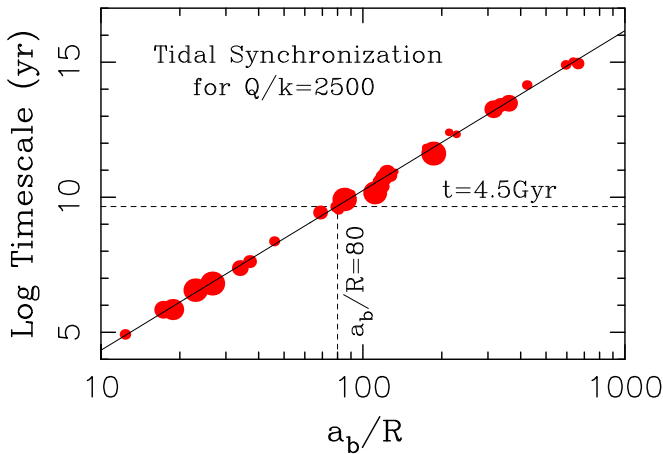


Figure 4. Tidal synchronization timescale τ_s for $Q/k = 2500$. We compute τ_s from Equation (2) for TNO binaries shown in Figure 2. The secondary spins are expected to be synchronized for up to $a_b/R \simeq 80$ over the age of the solar system (dashed lines). Also, the synchronization timescale is $\tau_s = 10$ Myr for $a_b/R \simeq 30$ and $\tau_s = 100$ Myr for $a_b/R \simeq 45$. For the nearly equal-size TNO binaries the primary components become synchronized on only slightly longer timescales. The density $\rho = 1 \text{ g cm}^{-3}$ was adopted here.

synchronous for $a_b/R < 80$ (Figure 2). To have $P_s > 100$ hr in a double synchronous state, $a_b/R > 12$. In summary, the spin periods $P_s > 100$ hr observed among Jupiter Trojans could be obtained from dissociated binaries with $12 < a_b/R < 30$ –45 and/or surviving binaries with $12 < a_b/R < 80$.

4. Binary Dissociation and the Yield of Slow Rotators

The outer disk lifetime is tied to Neptune’s migration. If Neptune’s migration started early (Ribeiro de Sousa et al. 2020), the disk was short-lived (e.g., $t_{\text{disk}} \sim 10$ Myr) and there was less opportunity for collisions to dissociate binaries. If the disk was long-lived (e.g., $t_{\text{disk}} \sim 100$ Myr), more binaries would become unbound by impacts. Binaries were also dissociated by dynamical perturbations during planetary encounters that occurred as bodies evolved from ~ 20 –30 au to 5.2 au (Nesvorný et al. 2018; Nesvorný & Vokrouhlický 2019). We determined the fraction of

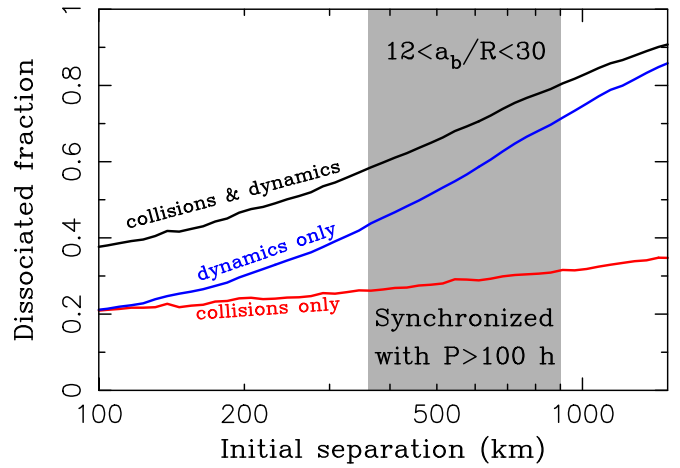


Figure 5. Dissociated fraction of equal-size binaries with $D = 30$ km in the case of short-lived outer disk ($t_{\text{disk}} = 10$ Myr). Different lines show the dissociated fraction as function of binary separation. The black line shows total fraction of dissociated binaries when both collisions and planetary encounters are taken into account. The shaded area denotes binary separations where binaries are expected to become synchronized over 10 Myr and have $P_s > 100$ hr. In total, 60%–80% of these binaries become dissociated and 20%–40% survive for $t_{\text{disk}} = 10$ Myr.

dissociated binaries using the methods described in Nesvorný et al. (2018) and Nesvorný & Vokrouhlický (2019). Here we first consider the case with $t_{\text{disk}} = 10$ Myr. Adopting $R = 15$ km as a reference value, we find that $\simeq 60\%$ – 80% of binaries with $12 < a_b/R < 30$ would be dissociated in this case (Figure 5). As planetary encounters provide the dominant dissociation channel, the components of dissociated binaries should maintain their original, presumably slow spin.

If we assume, for example, that $\sim 50\%$ of TNOs formed as binaries (meaning that $\sim 2/3$ of all individual TNOs were members of binaries; Noll et al. 2008; Fraser et al. 2017), \sim one-third of binaries had $12 < a_b/R < 30$ and became double synchronous, and $\simeq 60\%$ – 80% of binaries with $12 < a_b/R < 30$ were dissociated (Figure 5), then the expected fraction of slow rotators with $P > 100$ hr from dissociated binaries would be $\sim 2/3 \times 1/3 \times 0.7 = 0.16$. Here we conservatively assumed that all binaries with $a_b/R > 30$ became dissociated and contribute to singles. The fraction of slow rotators from dissociated synchronous binaries could thus explain observations (Ryan et al. 2017; Szabó et al. 2017). In addition, $\sim 30\%$ of binaries with $12 < a_b/R < 30$, and $< 20\%$ of binaries with $30 < a_b/R < 90$, would have survived for $t_{\text{disk}} \sim 10$ Myr, suggesting that at least some slow rotators may be surviving binaries. This possibility can be tested observationally.

In long-lived disks, binaries are predominantly dissociated by impacts (Nesvorný & Vokrouhlický 2019; their Figure 8). For example, $\sim 80\%$ – 90% of equal-size binaries with $R = 15$ km and $12 < a_b/R < 30$ would be dissociated for $t_{\text{disk}} = 30$ Myr. On one hand, the longer timescale would allow wider binaries to become synchronous and the larger dissociated fraction would increase the yield. On the other hand, a large number of impacts in long-lived disks would affect rotation (see below) and potentially remove any excess of slow rotators. This would have adverse implications for the overall yield of slow rotators. We thus see that the existence of slow rotators among Jupiter Trojans could be used to favor short-lived disks.

5. Spin-changing Collisions

Rotation of a small body can change as a result of impact. We tested this effect using the Boulder collisional code (Morbidelli et al. 2009). We assumed that the slow rotators have $P_s = 100\text{--}500$ hr initially and adopted the outer disk parameters from Nesvorný & Vokrouhlický (2019). A large uncertainty in modeling the effect of impacts consists in coupling of the impactor's linear momentum to the angular momentum change of the target (e.g., Dobrovolskis & Burns 1984; Farinella et al. 1992). This is because large and oblique impacts, which are the most important for spin changes, can eject substantial amounts of material in the direction of projectile's motion. Thus, only a fraction $f < 1$ of the projectile's momentum ends up contributing to target's spin. For $t_{\text{disk}} = 10$ Myr, we find that $\sim 55\%$ ($\sim 40\%$) of initially slow rotators with $P_s > 100$ hr and $D = 30$ km end up with $P_s < 100$ hr for $f = 1$ ($f = 0.3$).

If the spin-changing impact happens *before* a binary is dissociated, the spin can be re-synchronized by tides. If the spin-changing impact happens *after* the binary dissociation event, however, there is no way back to slow rotation via tides. We thus see that spin-changing collisions should reduce the net yield of the mechanism described here. The reduction factor will depend on the poorly understood coupling parameter f and t_{disk} , with larger reductions occurring for stronger coupling and longer disk lifetimes. Future experimental work and impact simulations could help to quantify f and help to disentangle effects of these two critical parameters. The spin-changing collisions become relatively rare *after* the implantation of bodies onto Jupiter Trojan orbits. Surviving binaries should therefore have ample time to tidally synchronize (and they do, as epitomized by the Patroclus-Menoetius binary).

6. Caveats and Outlook

The proposed model hinges on a number of assumptions. We adopted the capture model of Jupiter Trojans from Nesvorný et al. (2013), which is consistent with the orbital distribution and number of Jupiter Trojans, but other capture models are possible as well (e.g., Pirani et al. 2019). We assumed that the 100 km class TNO binaries with low binary eccentricities were circularized by tides and can therefore be used to infer the Q/k parameter. Moreover, we assumed that the estimated value, $Q/k = 1500\text{--}4000$, can be applied to small $D = 15\text{--}50$ km binaries as well.

Goldreich & Sari (2009) suggested that $k \sim 10^{-5}$ (R/km) for objects with rubble pile interior. Adopting this scaling here, the Q/k value inferred from circularization of tight TNO binaries would suggest $Q \sim 1$ for sizes considered here. This could mean that small TNOs can very efficiently dissipate the energy stored in the tidal distortion. For comparison, Goldreich & Soter (1966) found $Q \sim 10\text{--}500$ for the terrestrial planets and moons of the outer planets. Our interpretation implies that the TNO binaries with $a_b/R < 55$ should have synchronous rotation. This can be tested by photometric observations.

Additional uncertainty is related to the number of $12 < a_b/R < 30$ binaries that formed in the massive trans-Neptunian disk at 20–30 au. We know from observations of cold classicals that the overall binary fraction may have been high (e.g., Noll et al. 2008; Fraser et al. 2017; Nesvorný & Vokrouhlický 2019), but we do not know how high it was. These relatively tight binaries are difficult to detect observationally. To move forward, it would be desirable to identify

more slow rotators among Jupiter Trojans and in other small-body populations, and establish whether at least some of them are synchronous binaries.

The model discussed here could also explain slow rotators in the asteroid and Kuiper belts. The fraction of very slow rotators with $P_s > 100$ hr in the asteroid belt, and among Hildas in the 3:2 resonance with Jupiter, could be almost as high as the one found for Jupiter Trojans (e.g., Pál et al. 2020; Szabó et al. 2020). The equal-size binaries (e.g., the Antiope binary; Merline et al. 2000) may have formed in situ in the asteroid belt or been implanted (Levison et al. 2009; Vokrouhlický et al. 2016). The asteroid belt, however, is thought to have experienced rather intense collisional evolution (Bottke et al. 2005), implying very low chances of binary survival. Collisions have a profound effect on the spin distribution of asteroids as well (e.g., Farinella et al. 1992). In this light, it is intriguing that (253) Mathilde ($D = 53$ km) survived several large-scale impacts to end up with a very slow rotation ($P_s = 418$ hr; Mottola et al. 1995).

The work of D.N. was supported by the NASA Emerging Worlds program. The work of D.V. was supported by the Czech Science Foundation (grant 18-06083S). W.M.G. acknowledges support from NASA through grant No. HST-GO-15143 from the Space Telescope Science Institute, which is operated by AURA, Inc., under NASA contract NAS 5-26555.

ORCID iDs

David Nesvorný  <https://orcid.org/0000-0002-4547-4301>

References

- Batygin, K., Brown, M. E., & Fraser, W. C. 2011, *ApJ*, **738**, 13
 Bottke, W. F., Durda, D. D., Nesvorný, D., et al. 2005, *Icar*, **175**, 111
 Dobrovolskis, A. R., & Burns, J. A. 1984, *Icar*, **57**, 464
 Emery, J. P., Marzari, F., Morbidelli, A., et al. 2015, in Asteroids IV, ed. P. Michel, F. E. DeMeo, & W. F. Bottke (Tucson, AZ: Univ. Arizona Press), 203
 Farinella, P., Davis, D. R., Paolicchi, P., et al. 1992, *A&A*, **253**, 604
 Fraser, W. C., Bannister, M. T., Pike, R. E., et al. 2017, *NatAs*, **1**, 0088
 Fraser, W. C., Brown, M. E., Morbidelli, A., et al. 2014, *ApJ*, **782**, 100
 French, L. M., Stephens, R. D., Coley, D., et al. 2015, *Icar*, **254**, 1
 Gladman, B., Marsden, B. G., & Vanlaerhoven, C. 2008, in The Solar System Beyond Neptune, ed. H. Barucci et al. (Tucson, AZ: Univ. Arizona Press), 43
 Goldreich, P., Lithwick, Y., & Sari, R. 2002, *Natur*, **420**, 643
 Goldreich, P., & Sari, R. 2009, *ApJ*, **691**, 54
 Goldreich, P., & Soter, S. 1966, *Icar*, **5**, 375
 Grundy, W. M., Noll, K. S., Roe, H. G., et al. 2019, *Icar*, **334**, 62
 Johansen, A., & Lacerda, P. 2010, *MNRAS*, **404**, 475
 Johnston, W. R. 2018, Binary Minor Planets Compilation V2.0, NASA Planetary Data System, <https://sbn.psi.edu/pds/resource/binmp.html>
 Levison, H. F., Bottke, W. F., Gounelle, M., et al. 2009, *Natur*, **460**, 364
 Levison, H. F. & Lucy Science Team 2016, LPSC, **47**, 2061
 Marchis, F., Hestroffer, D., Descamps, P., et al. 2006, *Natur*, **439**, 565
 Medeiros, H., Lazzaro, D., & Kodama, T. 2018, *P&SS*, **160**, 77
 Merline, W. J., Close, L. M., Shelton, J. C., et al. 2000, *IAUC*, **7503**, 3
 Morbidelli, A., Bottke, W. F., Nesvorný, D., et al. 2009, *Icar*, **204**, 558
 Morbidelli, A., Levison, H. F., Tsiganis, K., et al. 2005, *Natur*, **435**, 462
 Mottola, S., Sears, W. D., Erikson, A., et al. 1995, *P&SS*, **43**, 1609
 Mueller, M., Marchis, F., Emery, J. P., et al. 2010, *Icar*, **205**, 505
 Nesvorný, D., & Vokrouhlický, D. 2019, *Icar*, **331**, 49
 Nesvorný, D., Vokrouhlický, D., Bottke, W. F., et al. 2018, *NatAs*, **2**, 878
 Nesvorný, D., Vokrouhlický, D., & Morbidelli, A. 2013, *ApJ*, **768**, 45
 Nesvorný, D., Youdin, A. N., & Richardson, D. C. 2010, *AJ*, **140**, 785
 Nolan, M. C., Howell, E. S., Scheeres, D. J., et al. 2019, *GeoRL*, **46**, 1956
 Noll, K., Grundy, W. M., Nesvorný, D., & Thirouin, A. 2020, in The Trans-Neptunian Solar System, ed. D. Prrialnik, M. A. Barucci, & L. Young (Amsterdam: Elsevier), 201

- Noll, K. S., Grundy, W. M., Chiang, E. I., et al. 2008, in *The Solar System Beyond Neptune*, ed. M. A. Barucci et al. (Tucson, AZ: Univ. Arizona Press), 345
- Pál, A., Szakáts, R., Kiss, C., et al. 2020, *ApJS*, 247, 26
- Parker, A. H., & Kavelaars, J. J. 2010, *ApJL*, 722, L204
- Petit, J.-M., & Mousis, O. 2004, *Icar*, 168, 409
- Pirani, S., Johansen, A., & Mustill, A. J. 2019, *A&A*, 631, A89
- Pravec, P., Harris, A. W., Vokrouhlický, D., et al. 2008, *Icar*, 197, 497
- Ribeiro de Sousa, R., Morbidelli, A., Raymond, S. N., et al. 2020, *Icar*, 399, 113605
- Ryan, E. L., Sharkey, B. N. L., & Woodward, C. E. 2017, *AJ*, 153, 116
- Stansberry, J. A., Grundy, W. M., Mueller, M., et al. 2012, *Icar*, 219, 676
- Szabó, G. M., Kiss, C., Szakáts, R., et al. 2020, *ApJS*, 247, 34
- Szabó, G. M., Pál, A., Kiss, C., et al. 2017, *A&A*, 599, A44
- Vilenius, E., Kiss, C., Müller, T., et al. 2014, *A&A*, 564, A35
- Visser, R. G., Ormel, C. W., Dominik, C., et al. 2020, *Icar*, 335, 113380
- Vokrouhlický, D., Bottke, W. F., Chesley, S. R., et al. 2015, in *Asteroids IV*, ed. P. Michel, F. E. DeMeo, & W. F. Bottke (Tucson, AZ: Univ. Arizona Press), 509
- Vokrouhlický, D., Bottke, W. F., & Nesvorný, D. 2016, *AJ*, 152, 39
- Vokrouhlický, D., Nesvorný, D., & Bottke, W. F. 2003, *Natur*, 425, 147
- Wong, I., & Brown, M. E. 2016, *AJ*, 152, 90